Full Paper

Propellants, Explosives, Pyrotechnics

DOI: 10.1002/prep.202000089

Short Pulse Initiation of an RDX-Based Explosive Using Large Diameter Flyer-Plate Impacts

Christopher Neel*[a] and Peter Sable[a]

Abstract: Ten impact experiments are presented that probe the initiation behavior of an RDX-based explosive. The explosive pellets were impacted by thin aluminum impactors supported by low-impedance polymers, thereby subjecting the pellets to short duration shocks. Impact conditions were used to determine impact tilt, pulse pressure and duration, sample transit time, and whether or not a detonation occurred. Exploding Foil Initiator (EFI) launchers were used as a baseline for evaluating the technique, and it was found that the present technique addresses multiple shortcomings of EFI-based systems. The aluminum foil allowed impacts with pressure durations of 70–80 ns, resulting in input conditions closely matching those of EFI-based systems. The thicker aluminum plate impactors resulted in pulse durations of approximately 600 ns and allowed access to a previously inaccessible region of the initiation curve. Initiation thresholds were bracketed using both impactors, and the data is compared with complementary initiation data from EFI-based systems with good agreement. Based on the results and closely related work, a novel, physically-based criterion is proposed to allow the initiation curve to be predicted based on the explosive's unreacted equation of state and sustained-pulse, shock-to-detonation run distance (the "Pop-plot"), giving a physical basis for previously published observations. Finally, the criterion is applied to the data available to propose a relationship between pressure, pulse duration, and run distance, suggesting that input pulse durations of 50–100 % higher than the critical condition should be applied to approximate the run distance of a sustained pulse.

Keywords: explosive · initiation · SDT · short pulse · attenuation criterion

1 Introduction

In military systems, it is commonplace for explosives to be initiated by pressure pulses resulting from high velocity impacts. These pulses are categorized as either "sustained" (held for a time longer than the initiation time) or "short" (held for a timeless than the initiation time). Other terminology includes "steady" for a sustained pulsed and "thin" for a short pulse. Sustained pulse initiation is typically described through a shock-to-detonation transition (SDT) criteria which specifies a distance required for a sustained shock wave of given initial pressure to traverse (run) before detonation will occur. Often, this is reported as a log-log relationship known as a Pop-plot, p. 313 of [1]. Pop-plot data is essentially infinite energy (due to the sustained pulse) initiation data and only correlates initiation with pressure (or power). This framework is well-established and important but does not describe a short pulse event. A short pulse will input less overall energy into an explosive system than a sustained pulse of equivalent pressure, and total energy is known to correlate with initiation. To account for the influence of both pressure (power) and energy (time held at pressure), James and colleagues developed more generalized criteria [2, 3]. They demonstrated that mechanical pulse detonation conditions could be posed in terms of power flux and transient energy fluence described by Eqs. (1) and (2).

$$\pi(t) = P(t)u_p(t) \tag{1}$$

$$E(t) = \int_0^{\tau} P(t)u_p(t)dt \tag{2}$$

In the equations, π is the time-dependent power flux equivalent to the product of pulse pressure, P, and shock-induced particle velocity, u_p. Energy fluence, E, is the integration of that flux over a characteristic time, τ, that is generally the duration of the input pulse. This formulation is able to incorporate the time-dependent nature of pulse energy deposition and is convenient in that all necessary values are already commonly measured. By observing initiation behaviour in these terms a critical energy threshold may be determined. It has been observed that a hyperbolic relationship of the form

$$\pi(t) = \pi_C \exp\left(\frac{-E_a}{E_C - E(t)}\right) \tag{3}$$

[a] C. Neel, P. Sable
Air Force Research Laboratory, Munitions Directorate
Damage Mechanisms Branch
101 W. Eglin Blvd
*e-mail: christopher.neel.1@us.af.mil
peter.sable.3@us.af.mil

describes the threshold for initiation, where E_C is the critical energy, π_C is the critical power, and E_a describes the transition between the two limiting cases. This criterion is often experimentally probed using an electrically-based miniature gun technique utilizing an exploding foil initiator (EFI). A high-power electrical supply, typically a capacitor bank, is used to explode a conductive foil. The resulting plasma drives a thin flyer, generally up to a few hundred μm thick and up to a few mm in diameter, at high speed into the explosive pellet being tested [4]. Upon impact the thin flyer imparts a short pressure pulse into the explosive. A critical threshold is then identified as the transition from a "No–Go" to "Go" detonation as impact velocity and/or flyer thickness increases. This approach has proven very useful, but has a few shortcomings. The small scale of EFI presents a great deal of practical difficulty in the characterization of impact conditions since parameters like flyer thickness, impact planarity (tilt), and impact velocity are based on characterization of the drive system rather than on measurements during the experiment. This results in a high level of experimental uncertainty, which can only be mitigated by doing many repetitions and applying statistics. Even so, this approach only mitigates the random thickness and velocity uncertainties, and these mitigated uncertainties remain important as discussed in the recent work of Bowden [5]. The combination of unknown flyer conditions (planarity, thickness, and velocity) with the small flyer diameter introduces systematic uncertainty and calls into question whether the initiation can be considered as a one-dimensional event.

The James (or HJ, for Hugh James) framework assumes ideal one-dimensional wave propagation. Gustavsen et al. [6] found that a thin-pulse did not affect run-to-detonation distance on PBX 9502 as long as the pulse was sustained for long enough that the shock wave did not attenuate prior to reaching the sustained pulse run distance. These were 1D experiments due to the large diameters and very planar impacts, and for this condition to apply, it is reasonable to assume that the diameter D must be large enough so that rarefactions from the edges do not reach the center of the advancing shock before the rarefaction from the back of the impactor of thickness h. Assuming that the leading edge of a radial rarefaction fan propagates inward at a speed U_R, the same rate as a longitudinal rarefaction fan would propagate forward, it is easily shown that the diameter must be at least 2 U_R h ($1/U_R + 1/U_S$). Applying an estimate of the relationship between U_S and U_R of $U_R/U_S \sim 1.3$, this amounts to an absolute minimum diameter of 4.6 h.

Very little experimental work examining the effect of impactor diameter on initiation is available. In the work of Kleinhanß [7], 100 and 250 μm thick Mylar™ impactors of various diameters were launched using an EFI apparatus, and the critical velocity was shown to stabilize as impactor diameter increased. This was done for several explosives, with sTable diameters ranging from 4 mm for PBXN-5, the most sensitive explosive tested, to 15 mm for cast TNT, the least sensitive tested. These findings resulted in a conclusion that a minimum diameter of 4 mm was needed for results that are independent of diameter. This represents a sTable diameter of >40 h, far exceeding the value of 5 h inferred from Gustavsen et al. Similarly, in the work of Honodel et al. [8] on ultrafine TATB initiated with 0.25 mm thick Mylar, the threshold velocity did not stabilize until the diameter reached 10 mm, again a ratio of 40 h. Furthermore, May and Tarver [9] reported data for LX-16 showing that at a flyer size of 0.7 mm x 0.7 mm and 0.025 mm thick (ratio of 28) the critical threshold velocity is still decreasing.

These subsequent findings using thin flyers indicate that much larger diameter-to-thickness ratios are needed than indicated by Gustavsen. There are several possible reasons for this, including conflation of the related but different metrics of "not affecting the SDT distance" with "causing a detonation", but another possible reason is that EFI results do not probe one-dimensional initiation except in the case of fairly sensitive explosives with small critical diameters. Since many initiation criteria (such as HJ) are 1-D theories, and because 1D experiments are useful to isolate the effects of 2D phenomena (such as critical diameter or corner turning effects) in more complex models, a need exists to be able to accurately access relevant power and energies in a 1D experiment. Furthermore, EFI can only launch flyers thinner than a few hundred μm and so produces only high-power, low-energy fluence, conditions. This prevents lower power, higher energy regimes from being explored, and effectively bars experimentally linking the short pulse and steady pulse regimes while maintaining 1D boundary conditions.

There are a few fleeting references to such a capability in the literature, where large diameter, thin flyers are launched. The work of Tarver and May [10] is one, where they report Mylar and aluminum flyer thicknesses ranging from 0.05 mm up to 1 mm with 25 mm diameters launched from electric guns that explode a metal foil to launch a flyer. The paper concentrates on the model development for TATB and most of the corresponding experimental details are given in earlier works by Honodel et al. [8] and Weingart et al. [11]. Honodel describes a single experiment with a flyer-plate diameter of 3.4 mm and that of Weingart mentions up to 2.5 mm. Overall the EFI data seems limited to about 1.25 mm thick flyers for reasons that are not clear. The paper by Weingart includes a useful discussion of limitations and trade-offs inherent to the EFI technique, but they do not discuss the upper limits of flyer thickness, presumably because the relatively long-duration pulses produced by the thick flyer were simply not the focus of the study. Trott and Jung [12] used a 100 mm diameter explosive plane-wave generator to launch large diameter flyers of various thicknesses into several explosives, most notably Comp-B. The study was extensive and although the authors are not specific about the diameters, the illustrations and text suggest diameters of 25–50 mm and flyer thicknesses from 0.2 mm up to over 4 mm. The difficulty and limitations of this approach are also illustrated, with discussion indicating

that spallation limited the thicker flyers to relatively low velocities and other discussion alluding to significant development required to modify the launch conditions. Nevertheless, it was Trott and Jung's clear intention to connect sustained-pulse Pop-plot data to short-pulse initiation data in much the same way that the present authors hope to do with the technique outlined in the present work.

The prevalence of short pulse ignition in military fuzing motivates addressing these issues in order to improve the understanding of initiation and the ability to correctly predict whether it will occur in various circumstances. The work herein details an alternative test methodology which utilizes a flyer-plate impact approach on a large diameter (60 mm) single-stage powder gun to input one-dimensional pulses into RDX-based explosive pellets with durations ranging from short (less than 100 ns) to sustained (greater than 1 μs). The technique addresses virtually all of the shortcomings discussed above, allowing large ranges of impactor thickness, known impact velocities, known pulse durations, and verifiable planarity, all while maintaining one dimensionality. Resulting observed waveforms demonstrate the production of near-ideal one-dimensional pulses with quantifiably low uncertainty. Varying flyer thickness enabled the investigation of low-power / high-energy ignition behavior, previously unavailable. "Go" vs "No–Go" detonation behavior was determined over a range of impact pressures and two flyer thicknesses, which is used with other data to estimate an initiation criteria using a modified HJ framework. The criteria is then used to draw larger conclusions about the relationship between HJ parameters and run distance.

(a)

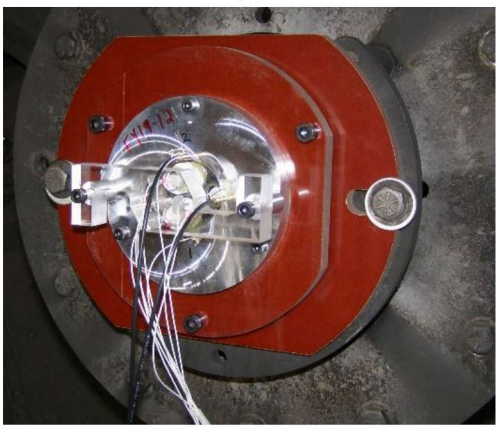

(b)

Figure 1. (a) The HP3 facility local at the AFRL Munition's Directorate at Eglin AFB. The picture is the 60 mm powder gun leading into the containment chamber. (b) A short pulse experiment target mounted just downrange from the muzzle within the containment chamber. The view is from downrange, such that the muzzle is behind the target.

2 Experimental Setup

2.1 Overview

A series of ten flyer-plate impact experiments were conducted utilizing the 60 mm single stage powder gun at the AFRL Munition Directorate's High-Pressure Particulate Physics (HP3) facility on Eglin AFB. Each experiment consisted of a gun-driven, flat-faced projectile impacting a target assembly mounted at the muzzle. Figure 1 shows the 60 mm gun as well as a mounted target assembly.

Flyer-plate impact experiments rely on the precision alignment of the flat-faced target with respect to the incoming flat-faced disk projectile. The large diameter ensures one-dimensional shock wave propagation into the center of the target due to inertial confinement from the edges. The duration of the pulse is controlled by the thickness of the flyer. Figure 2 depicts the flyer-plate impact configuration employed in this effort. Figure 2 shows a mid-sectioned schematic view of both projectile and target just prior to impact, while Figure 2b is an X-t diagram which visualizes expected wave propagation, and demonstrates how the thickness of a given flyer controls pulse duration. The plot is representative of an actual experiment and shows the case for a 0.251 mm thick aluminum flyer which induces a pulse lasting approximately 75 ns. For this example, the leading edge of the release wave overtakes and attenuates the shock beyond about 1 mm into the sample.

Figure 2 shows a simplified 2D representation of the experiment. In the actual experiment, there were two HE pellets and a blank, shown in Figure 3. What follows is a discussion outlining the material and assembly procedures pertaining to the target and projectile respectively, with individual components described.

2.2 Target

The target assembly consisted of three cylindrical specimens, two explosive and one inert surrogate, held within a polymethylmethacrylate (PMMA) trefoil holder ring, which

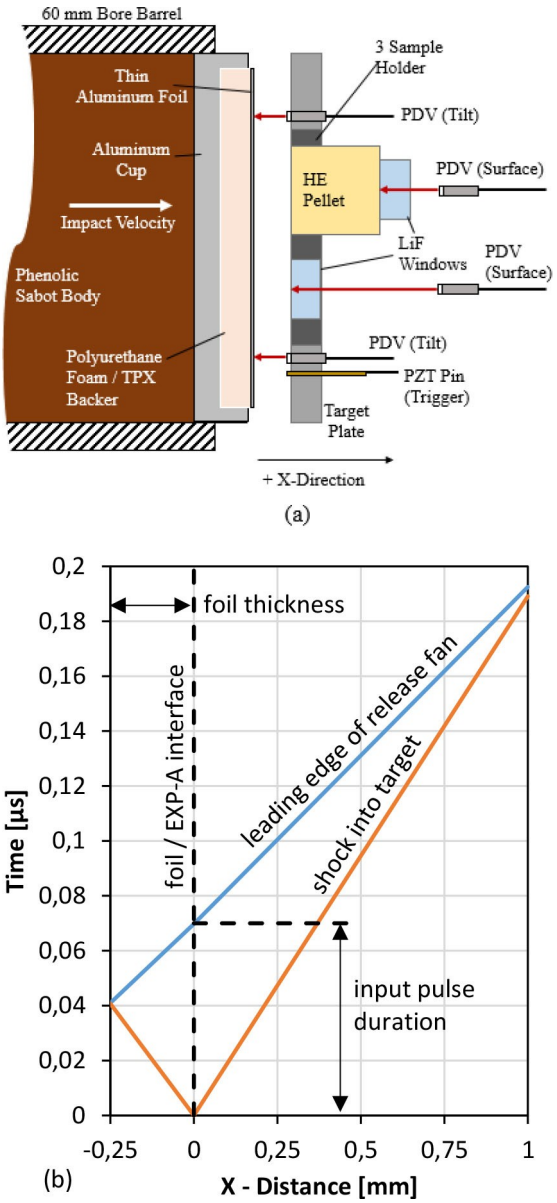

Figure 2. (a) A schematic cross-section view of the flyer-plate setup, note each target consisted of two HE pellets (only one shown) and a LiF target surrogate. (b) X-t diagram of shock propagation, demonstrating the kinematics of inducing a short duration pulse and approximating release as a single wave rather than a dispersed fan.

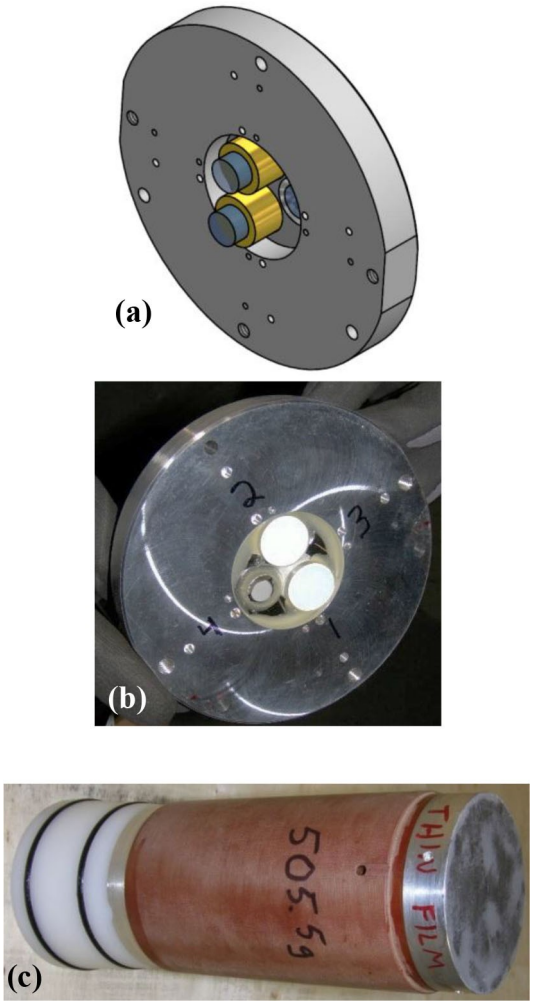

Figure 3. (a) Rendering of the designed target assembly including both explosive pellets (gold) backed by LiF windows (blue). The view is from the rear. (b) Photo of the impact face of a target assembly. Here the explosive appears white and the view is from the front. (c) An assembled projectile for use in short pulse flyer-plate impact experiments. The aluminum foil impactor supported by a backer can be seen contained within an aluminum cup which is further mounted to the sabot (brown phenolic body with white HDPE obturator).

was all contained within a mounTable 6061-T6 aluminum target plate. Explosive specimens were fabricated by AFRL. The explosive is a cast-cure explosive formulation consisting of 89% RDX and 11% lauryl methacrylate (LMA) hereafter referred to generically as explosive A, or EXP-A. The samples were cast as "stick" cylinders of 19.05 mm nominal diameter, and then cut and machined into pellets 19.05 mm long. Precise densities of specimens used in this study could not be determined due to uncertainty in the outer diameter of the pellets. This uncertainty was caused by an exterior layer (~1 mm thick) of oxidation which complicated diameter measurements and interpretation. However, beyond complicating the density determination, the oxidation layer is assumed irrelevant to data interpretation moving forward since the machined flat faces did not have this layer. Since no measurements were available, densities were estimated to be 1.604 g cm^{-3} in agreement with Lacina et al. [13].

The inert surrogate consisted of optically transparent lithium fluoride (LiF) cylinder, 12.7 mm diameter, and 6.35 mm thickness, cut so that the faces were [100]. The LiF cylinders were also used as "backers", i.e. they were attached to the rear (downrange) face of the explosive pel-

lets. This was achieved by placing them on the pellets under light weights, daubing 2-part epoxy on 2–3 spots around the periphery of the interface, and then allowing the epoxy to cure before removing the weights. This setup avoided a film of air becoming trapped between the sample and the LiF in a vacuum environment, but no clamping device was utilized in the completed target. The lack of clamping together with the surface roughness of the pellet makes it virtually assured that a film of rarefied air (at 13.3 Pa) was present at portions of the interface. This unquantified complication was ignored in analysis. LiF window backers were coated with aluminum to allow for the necessary reflection of laser diagnostics. Figure 3 shows both a representative target design and a final assembly just before experimentation. Photon Doppler Velocimetry (PDV) was the primary diagnostic used, wherein 1550 nm laser light is emitted toward a target surface of interest, and any motion of the target shifts the frequency of reflected light which is then captured and used to infer surface (particle) velocity [14]. A total of eight separate PDV channels were used for each shot with light emitted and collected through fiber-optic collimators. Two looked at the center of the rear surface of each EXP-A sample, through the optically transparent LiF windows. A third looked through the LiF target surrogate, viewing the impact surface directly, and a fourth looked along the shot centerline, through the PMMA trefoil holder. The remaining PDV channels were placed symmetrically around the outer diameter of the target within the mount plate and were used to measure the incoming projectile velocity, impact time, and tilt.

Impact tilt should be considered with some amount of skepticism since values reported hereafter are given with respect to the target plate and not the explosive pellets themselves. When inserting explosive pellets into place, it was not feasible to prevent small flakes of oxidized powder from falling, causing the sample impact faces to be offset from the surface of the target plate. Also, the flatness of the machined surfaces (ignoring the powder) was not measured due to time constraints for measurements on explosives. Due to these reasons, no tilt measurements were made of the pellets with respect to the target plate. Future sample fabrication or target assembly improvements could remedy this issue. Hereafter, it is assumed that the impacted pellet faces were coplanar with the target plate they were mounted into.

2.3 Projectile

Targets were impacted by a projectile composed of a thin aluminum disc on the impact surface (the flyer) which was supported by a low impedance polymer disc (the backer), all contained in an aluminum cup that was on the front of a projectile. The backers support the flyer during launch acceleration but are low impedance so that after impact, the pressure is relieved upon encountering the interface, limiting the duration of the pulse into the target. Two variants of aluminum flyer were used, either foil or a thin disk cut from a sheet. The aluminum foil was purchased from All Foils, Inc. as a roll of 1235-O Al alloy with a nominal thickness of 0.25 mm. The thickness was measured and found to be consistently 0.251 mm. In most experiments, the foil was not further lapped or prepared, but in the first experiments some light hand polishing was attempted on the impact face after the projectile was assembled. Aluminum discs were obtained as 6061-T6 aluminum sheet that was cut into discs and then lapped to a final thickness of approximately 1.743 mm. The backer for the foil was rigid polyurethane foam (General Plastics FR-4515), cut into discs. The first three experiments used 6.35 mm thick foam, but the thickness was increased to 12.7 mm thick after the first three shots for reasons mentioned later. The backer for the thicker plate configuration was polymethylpentene (TPX). All impactors and backers were 55 mm diameter. Figure 3 shows a typical completed projectile. Light polishing was attempted and resulted in the uneven appearance of the impact surface.

3 Experimental Results

Data collected from each shot consisted of a collection of PDV velocity histories ("traces") from locations previously described. Results from these measurements were analyzed in an effort to accomplish two broad objectives. The first is to evaluate the technique and the "quality" of the impact, by which is meant the one-dimensionality and associated uncertainty. The second is to present the initiation data on EXP-A; namely, the input shock magnitude, duration, and detonation or lack thereof. The section is therefore organized under these two objectives.

3.1 Impact Quality

An original objective of this technique was to improve on aspects of the EFI setup specifically with respect to uncertainty, dimensionality, and range. Aspects of the former two characteristics are perhaps best understood through the quantification of tilt and the more precise knowledge of impactor dimensions and impact loading conditions.

Tilt at impact was quantified by measuring the skew between the target reference plane and the impact plane at, or just prior to, the moment of impact. The target is measured prior to the shot to determine the protrusion of four PDV probes with respect to the target plane (typical protrusion is 25–50 μm, measured to <1 μm, uncertainty of 5 μm). Velocity profiles from each probe observe the incoming projectile velocity, and the time at which the GRIN lenses are impacted is assumed to correspond to a characteristic drop in the apparent velocity that can be assigned an arrival time to within a few ns.

From observed arrival times and corresponding location information, a plane is found with some skew relative to the target plane. The skew is assumed to persist over the very small distance between the probe tips and the target such that the skew represents impact tilt. Typically, this procedure is applied to the sample target face, but as previously discussed, in this case, it was performed with respect to the aluminum target plate. Impact tilt thus calculated was consistently less than 10 mrad (with respect to the target plate).

The tilt calculation uses four points (one from each of the four PDV probes devoted to impact velocity and impact time), which over constrains a plane. The degree to which all four points fit the plane is a measure of the quality of the impact, and in all cases in this work the agreement was excellent, indicating no undesirable impactor deformation. However, all four points were at the periphery of the round impactor, and so a curved shape such as a sphere could also be interpreted as a plane. Since the curvature was a concern with the foil/foam impactor, the impact time at the center of the acrylic trefoil holder was also used (along with the measured height) to determine the curvature of the impactor assuming a spherical deformation. This is described by Eq. (4).

$$r = \frac{1}{2h}\left[\left(\frac{D}{2}\right)^2 + h^2\right] \tag{4}$$

Where r is the radius of curvature, h is the calculated center protrusion of the sphere, and D is the impact surface diameter. Once r is obtained, an angle θ is calculated, representative of the tangent of the sphere at the diameter edge with respect to the impact plane. The result is a conservative estimate for potential tilt contribution from flyer curvature, stated in Eq. (5).

$$\theta = \sin^{-1}\left(\frac{D}{2r}\right) \tag{5}$$

Ten experiments were conducted. Table 1 details various relevant parameters which quantify potential tilt contributions within the conducted short pulse flyer-plate impact experiments. All times shown are with respect to the shorting pin diagnostic trigger time. From the calculation of the worst-case tilt from curvature in the last column, it is clear that the curvature of the impactor is very small. This finding, together with the good planar fit of the four peripheral point, indicates a low-tilt, very planar impact even with aluminum foil that is 55 mm diameter and supported by foam.

A last aspect regarding dimensionality concerns the imparted wave pulse. Figure 4 displays all the LiF surrogate traces overlaid. Waves from both flyer thicknesses, with durations of roughly 75 or 580 ns respectively, show clean profiles followed by immediate release. The thicker impactors backed by TPX do not release as completely as those backed by the foam, but the release is still sufficient to decrease the power below a level that is expected to contribute to initiation.

In examining Figure 4, the range of available impact conditions becomes apparent, limited only by available impact velocities and availability of flyer thicknesses. Pulse durations are repeaTable and predictable. This enables a large parameter space to be explored and allows unique access to the low-power, high-energy space previously inaccessible through EFI. Overall, the technique has far less uncertainty due to the precise measurement of impact velocity, known pulse durations, and verifiable tilt and planarity. The dimensionality is known to be 1D (to the extent allowed by the pellet diameter) by virtue of the impactor covering the entire diameter of the pellet. The range in HJ space is practically limited only by the upper limit of impact velocities. Overall, measured conditions demonstrate the impact quality of the technique is very good and substantially exceeds that of the EFI impacts in the three areas of uncertainty, dimensionality, and low-power – high-energy range.

Table 1. Relevant parameters quantifying impact tilt, including potential curvature of the thin aluminum impactor. Overall tilt is given with respect to the target plate, and the PMMA holder is assumed flush with the same.

Shot ID	Impact |Tilt| mrad	PMMA Holder Center Protrusion mm	Projected Impact Time at Center μs	Center PDV TOA μs	Impact Velocity mm/μs	Radius of Curvature, r mm	Estimated Tilt from Curvature mrad
FY19-06	3.2	0*	0.618	0.632	1.876	−44497	−0.62
FY19-07	8.9	0*	0.372	−0.0565	1.644	1238	22.21
FY19-08	2.2	0*	0.266	0.313	1.360	−9374	−2.93
FY19-11	2.0	0*	0.305	0.235	1.879	8622	3.19
FY19-22	16.9	−0.04	0.331	0.292	2.167	18137	1.52
FY19-25	2.2	0.01	0.248	0.213	1.067	9870	2.79
FY19-29	5.5	0.015	0.321	0.219	2.317	7328	3.75
FY19-12	2.2	0*	0.236	0.235	2.417	599751	0.05
FY19-23	9.1	0.004	0.445	–	1.373	–	–
FY19-24	5.5	−0.082	0.324	0.387	1.181	−6054	−4.54

*No measurements were taken, so the value was assumed zero for computations. Curvature values should be treated with skepticism.

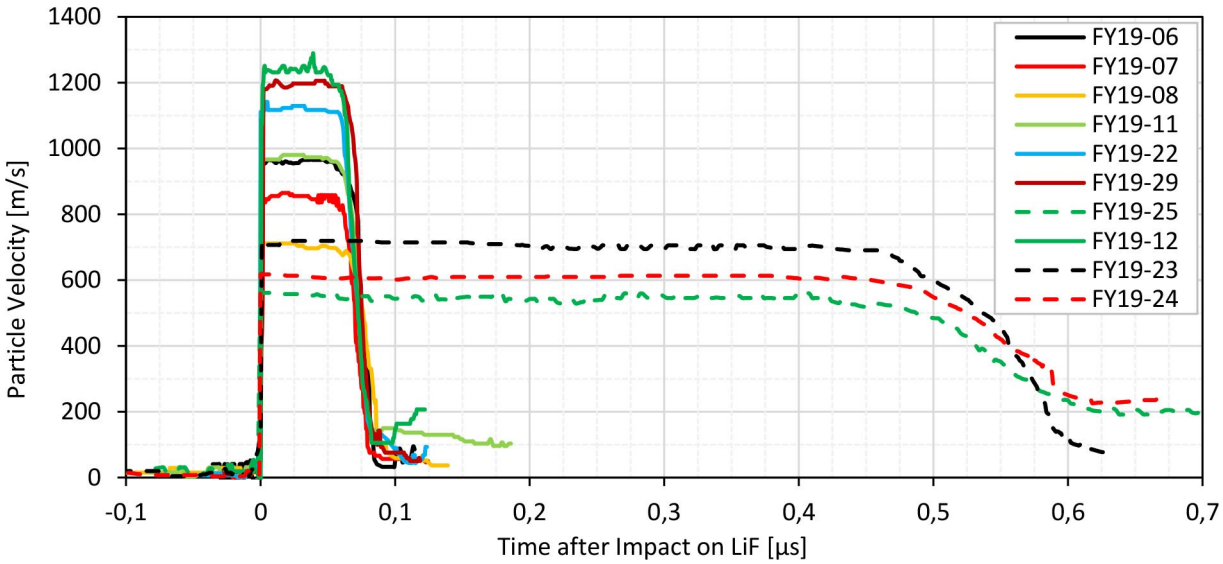

Figure 4. The measured short pulse waves imparted during each experiment. Input pulses were approximately either 75 or 580 ns in duration.

3.2 Input Shock and Detonation Determination

In order to infer the HJ conditions (primarily the pressure and particle velocity in Eqs. (1) and (2)) inside the EXP-A for each experiment, impedance matching calculations were performed using the Rankine-Hugoniot conditions and the known impact velocity [1]. This required the assumption of an unreacted EXP-A Hugoniot of the form $U_s = S^*u_p + C_0$, where parameters $S = 3.32$ and $C_0 = 1.25$ km/s [13]. Impedance matching enabled the determination of U_s, P, and u_p, and the latter two directly inform Eqs. (1) and (2). Pulse duration is then found from shock speed, release wave speed, and flyer thickness assuming Eq. (6).

$$\tau = \left(\frac{h}{U_s}\right) + \left(\frac{h}{U_R}\right) \tag{6}$$

Time duration τ is a function of flyer thickness, h, shock speed, U_s, and rarefaction wave speed, U_R. Rarefaction wave speed is approximated using the same Hugoniot constants through the relation $U_R = C_0 + 2Su_p$. As discussed later, this calculation of U_R is arguably too high, but in the case of these impactor materials, the over-estimation is small. The determination of U_S, pressure, u_P, τ, and tilt provide a reasonably complete characterization of the imparted pulse. These values could not be determined from experiment alone as only the velocity history of the LiF interface was recorded with PDV. The slightly higher impedance of the LiF target compared with the explosive results in slightly higher pressures, but the observed traces still allow good characterization of the input pulse through impedance-matching techniques and the relative closeness of the impedances of all three materials involved (LiF and Al have virtually identical impedances, and are both only slightly higher than unreacted EXP-A).

For all PDV data based on transmission through LiF, an optical correction factor was applied to determine actual (as opposed to apparent or uncorrected) velocities. The correction used was actual equal to apparent/1.267, determined from the data of Jensen et al. [15]. Figure 4 shows traces from the LiF surrogates in all experiments. The pulse into the LiF surrogate has a clean rise and constant top, indicating an abrupt rise to a constant pressure that is maintained for approximately 75 ns before releasing to near zero. This is in good agreement with impedance matching based on aluminum and LiF Hugoniots, which estimate an expected duration of 72 ns for a 0.251 mm thick flyer and a resulting particle velocity of 1231 m/s. The duration of the release corresponds to the rarefaction fan that is inherent to most materials, and in these experiments with foil impactors is roughly 20 ns. The pulse does not release completely to zero due to the presence of the foam backer, but the release is almost complete, and more than sufficient to drop the pressure down below where it is expected to contribute to detonation in a HJ initiation framework (well below π_C). This low level is maintained for approximately 900 ns (for the 0.251 mm foil configuration with PU foam) or 500 ns (for the 1.745 mm plate configuration with TPX). The wave is representative in appearance of other tests with foil impactors and demonstrates the ability to input near-ideal pulses. Based on the assumed Hugoniots for unreacted EXP-A and aluminum, the pressure in the explosive for the experiment shown in Figure 5 was 15.23 GPa.

Identification of a detonation (a "go") or lack thereof (a "no-go") was based on examination of the PDV traces from the EXP-A/LiF interfaces. A go was apparent when a classic

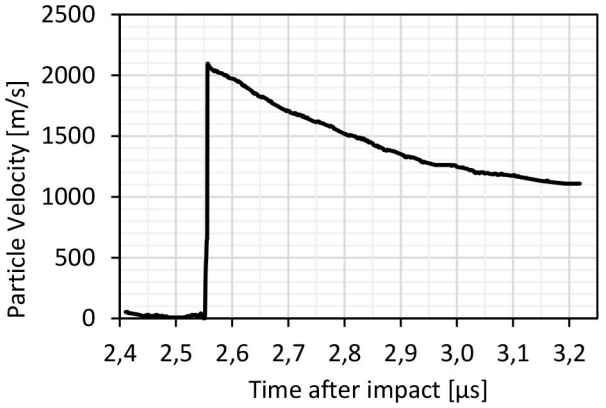

Figure 5. A velocity history taken at the rear of an EXP-A pellets (at the LiF interface) for a typical "go" shot, FY19-12. The velocity has been corrected to account for the index of refraction of LiF. Profiles such as these are indicative of detonation waves.

Taylor wave could be observed. A typical "go" trace is shown in Figure 5, and at least one of the two PDV probes in each experiment recorded a trace such as this for each "go" result. Multiple other indicators made go/no-go determinations unambiguous, including the transit time through the pellet (it was much less in cases of a go), and velocity magnitude at the rear (free) surface of the LiF (it was far higher in the case of a go).

Two different regimes of energy fluence were investigated by using two distinct aluminum impactor thicknesses. The lower energy regime was accessed using the foil impactor and was comparable to the energy and power of exploding foil studies, while the higher energy was accessed using the thicker plate impactors and is previously unexplored. Varying impact velocity primarily varied input power (with a slight effect on τ). A series of shots were done at each regime in order to bracket a threshold for each case. Of all experiments, four resulted in detonation. Table 2 summarizes relevant shot impact conditions for all experiments, including descriptions of the imparted pulse and the "Go" (detonated) or "No–Go" (did not detonate) result. Due to difficulties with sample placement described previously (due to chalky debris from the outer diameter of the sample), impact time on the sample faces could not be sufficiently defined to allow for meaningful computation of the transit time, and so no transit time or shock-detonation transition distance is shown in the table.

4 Discussion

Up to this point, the impact quality produced by the technique has been discussed and experimental results have been presented. The focus shifts here to interpreting the data as an initiation threshold, using the threshold in conjunction with related work to propose a criterion for initiation, and discussing the implications of the threshold criterion.

4.1 Comparison with EFI Threshold Data

Laboratory-scale EFI data on ostensibly identical (same recipe but different batches) EXP-A pellets is available [16]. The data was obtained with an EFI apparatus launching 12.7 mm diameter flyers of polyimide. The velocity and impact pulse duration was characterized using a statistical approach with multiple trials at a given geometrical configuration and drive-current into a transparent surrogate target allowing for direct measurement of the impact velocity via a PDV probe looking through the surrogate, in a manner perfectly analogous to that used in the present work with the LiF surrogate. Once the parameters were tuned and a velocity established, the surrogate was removed and a pellet identical to that used in the present

Table 2. Summary of flyer-plate impact experiments used to investigate the short pulse ignition behavior of EXP-A. Included are relevant initial impact conditions as well as imparted pulse duration, pressure, wave particle velocities, and the final "Go" / "No–Go" result. For "Go" experiments, average transit speeds are shown as a convenient physical check (the average speed should be between the shock and detonation speed).

Shot ID	Backer Material	Impactor Thickness mm	Impact Velocity mm/μs	Pulse Duration τ μs	Pulse Pressure P GPa	Particle Velocity u_p mm/μs	Go/No-Go
FY19-06	PU Foam	0.251	1.876	0.077	10.61	1.236	No-Go
FY19-07	PU Foam	0.251	1.644	0.079	8.73	1.105	No-Go
FY19-08	PU Foam	0.251	1.36	0.082	6.61	0.940	No-Go
FY19-11	PU Foam	0.251	1.879	0.076	10.64	1.238	No-Go
FY19-22	PU Foam	0.251	2.167	0.074	13.16	1.396	No-Go
FY19-25	TPX	1.743	1.067	0.589	4.66	0.763	No-Go
FY19-29	PU Foam	0.251	2.231	0.072	14.56	1.478	Go
FY19-12	PU Foam	0.251	2.417	0.072	15.52	1.531	Go
FY19-23	TPX	1.745	1.373	0.567	6.70	0.948	Go
FY19-24	TPX	1.743	1.181	0.581	5.39	0.833	Go

work was inserted, and then several experiments were performed at identical settings to establish whether or not the point was a detonation or not. This procedure was performed with three different geometric configurations 50 μm, 125 μm, and 250 μm thick polyimide flyers, each with a different velocity, resulting in three points in HJ space (or in P- τ space).

The data of Table 2 can be readily plotted in P-τ space. Recalling Eqs. (1) and (2), HJ space parameters can be quickly calculated from the tabulated values of pressure, particle velocity, and pulse duration. When integrating over time to find energy fluence, pressure was assumed constant. This was considered reasonable given the constant nature of the Hugoniot state observed within each pressure pulse, and a more detailed numerical integration was found to make little difference. The EFI-based data used the same approach in calculating pulse parameters so it is directly comparable. A comparison of the data of this work and the EFI data are shown in both P-t and π-E (power-energy) in Figure 6. The Figure also shows notional threshold lines between the initiation region ("det." in the figure) and the failed initation region ("no det." in the figure).

Given the limited data available, the results from the new gun-driven technique are in good agreement with the EFI results at similar power flux. This provides some verification of the new methodology. The EFI technique is generally unable to access the portion of the initiation curve at lower power/pressure and higher energy/pulse duration (shown circled in grey in the figures), and so the data from the new technique represents the first data ever available in this region. The agreement indicates that the EFI results are not affected by two-dimensional phenomena, and is essentially probing 1D shock to detonation. This is perhaps unsurprising, since at 15 GPa the Pop-plot of Lacina [13] indicated a run distance of less than 2 mm, and the diameter of the EFI experiments was 12.7 mm. However, some influence of diameter would be expected as the diameter decreases toward 5–6 mm.

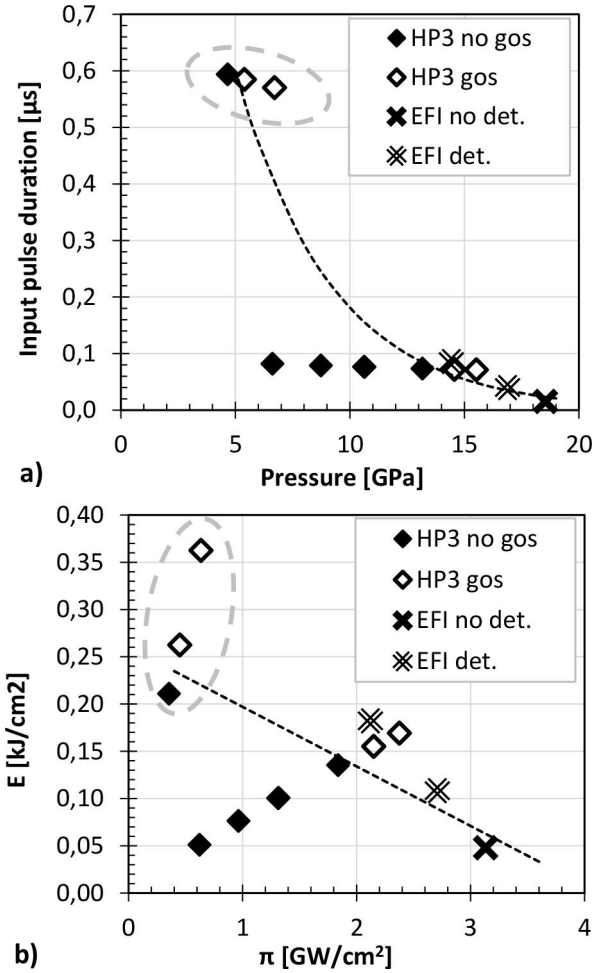

Figure 6. Comparison of this work (denoted "HP3") with available results from EFI detonators on EXP-A, along with notional threshold curves separating the detonation region from the failed detonation region. The limited data set suggests good agreement between the techniques. The data circled represents a region of the initiation space that is essentially inaccessible by other laboratory techniques. (a) Pressure/impulse duration space, with exponential threshold, (b) power/energy space, with linear threshold.

4.2 Proposed "Attenuation Criterion" for Initiation

The observations of Gustavsen [6] and Lacina et al. [13], whereby thin-pulse run distances are identical to those of sustained pulses as long as the shock is not attenuated, can be considered as an initiation criterion and mapped in H-space, thereby linking the pop-plot and initiation curve. The construction shown in Figure 7 illustrates the concept, where the intersection between the shock and release (approximated as a single wave) occurs at a critical distance x_c and critical time t_c and varies based on the duration of the input pulse τ. The slopes of the shock and release lines in the plot are the inverse of the shock velocity U_s and the release velocity U_R. Due to the close impedance match of aluminum and EXP-A, the speeds in the foil and explosive are visually indistinguishable in the Figure but, in general, these slopes are not similar. It is worth noting the implicit assumption that the shocked explosive into which the release wave is travelling is still represented by the unreacted explosive, even though the explosive is beginning to react and so perhaps some treatment of release wave speed in a partially reacted mixture is warranted. Since the amount of reacted material is small until just before final transition to detonation, and because the *increase* in sound speed due to the slow increase in pressure is somewhat counteracted by a *decrease* due to the lower wave speeds of the products (assuming pressure equilibrium), this complication is ignored.

It is straightforward to show that $x_c = \tau/(1/U_s - 1/U_R)$. Using the standard form of a Pop-plot, $\log(x_D) = A + B \log(P)$, where x_D is the run distance for SDT of a sustained pulse of

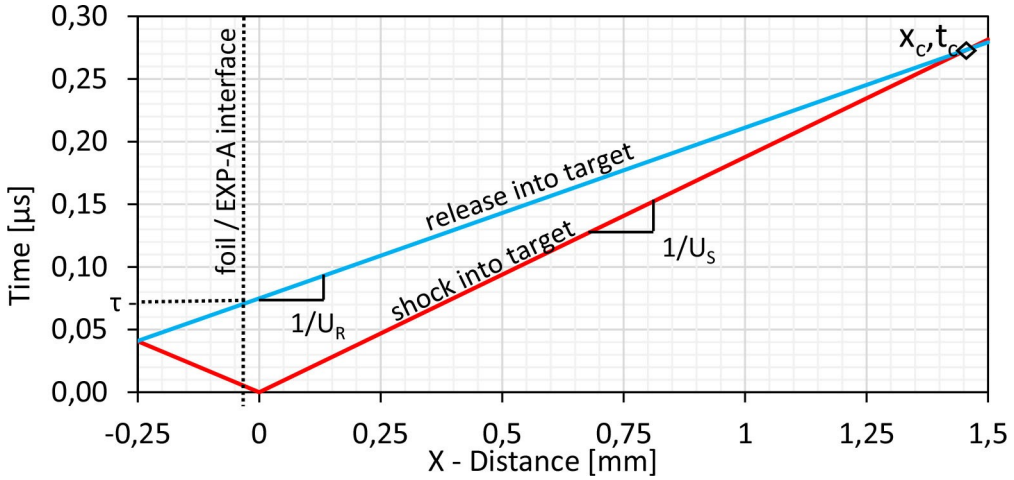

Figure 7. Illustration of shock and release into an explosive, highlighting the pulse duration τ and the critical distance x_c and time t_c until the rarefaction attenuates the shock. The construction is formulated for shot FY19-06 and uses $U_R = c_0 + 1.5*S*u_P$ for release wave velocities.

pressure P, and A and B are constants for a particular explosive, the criterion $x_c = x_D$ may be applied. In other words, the criterion is that initiation at an input pressure P will occur if and only if the impulse duration τ is sufficient such that the pulse is not attenuated at a depth equal to the run distance $x_D(P)$. Substituting and slightly rearranging, this is stated mathematically as

$$\log(\tau) = \log\left(U_S^{-1} - U_R^{-1}\right) + A + B\ log(P) \tag{7}$$

The Hugoniot of the material can be used to calculate $U_S(P)$, but the $U_R(P)$ relationship is less straightforward since the release wave is a dispersed fan rather than a shock. The leading edge of the release wave depends on the slope of the isentrope from the shocked state, which in turn requires thermodynamic data that is not typically available, and so it is preferable to use a simpler formulation. The slope of the isentrope at a state can be estimated as the average of the slope of the Hugoniot and the slope of the Rayleigh line (p. 28 of [17]), and then used to estimate the bulk sound speed which (in the absence of material strength) defines the leading edge of the release fan. Other sources occasionally use the slope of Hugoniot, p. 227 of [1], which results in very high release wave speeds and is not utilized here. Even a simple fixed ratio to the shock speed can be used as a crude release wave speed estimate, and $U_R = 1.3*U_S$ is examined here (this is a common but unpublished "rule of thumb" estimation used to design shock experiments (in Lagrangian coordinates)).

Regardless of the method by which U_R is computed, formulating $U_R(P)$ allows for the criterion $x_c = x_D$ to be expressed in the form of τ(P) for a particular explosive as shown in Eq. 7. This dependency can be plotted directly or used to create any of the common initiation curves such as power ($P*u_p$) vs energy ($P*u_p*\tau$). Figure 8 shows the experimental data as well as the estimated initiation curve using the new pop-plot-derived initiation criteria computed with two different approximations for $U_R(P)$ and Pop-plot data (A = 2.06, B = −1.52 from [13]).

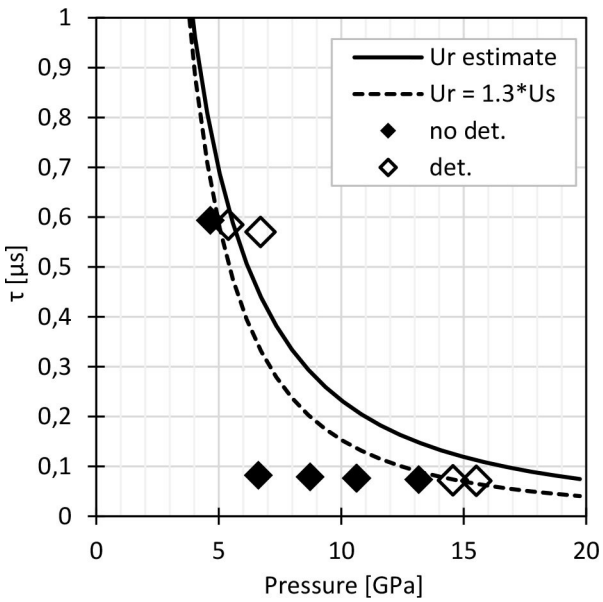

Figure 8. Experimental data vs predictions from the Pop-plot-based attenuation criterion, using two methods of estimating the release velocity U_R: from the average of the Hugoniot and Rayleigh line slopes (solid line) and from a simple fixed ratio (dashed line). The dashed line neatly divides the detonation from the "no detonation" data and so is a potential threshold description.

From inspection of Figure 8, it is apparent that using a $U_R(P)$ formulation that results in a U_R/U_s ratio of 1.3 leads to very close agreement with the experimental data previously introduced and discussed. Using the estimate of the leading edge results in higher estimates of U_R (ranging from 1.38 U_s at 5 GPa to 1.65 U_s at 15 GPa) and worse agreement. That

better agreement is obtained with a somewhat artificially lower estimate of U_R is not surprising. It is physically plausible that the theoretical leading edge of the release wave is not the appropriate value to use to calculate the time duration τ, since a negligible drop in pressure should not affect the initiation.

While some more complex integration method could be investigated, or some scheme whereby τ is set based on the time at which the pressure is within some fraction of the peak pressure, the idea that some intermediate value of the release velocity, rather than the leading edge, should be used to calculate τ makes sense. Therefore, the use of a single physically-based "fitting parameter" is reasonable and allows a convenient way of estimating the initiation curve from the Hugoniot and Pop-plot if no other initiation data is available. For EXP-A, estimating U_R as 1.3*U_s seems to suffice. Although the above discussion is framed in P- τ space due to that being the simplest explanation of the criterion, the same criterion is easily applied to, for instance, power flux and energy flux space, with similarly good agreement.

If the "attenuation criterion" is accepted as generally applicable, it implies that the same 1D physics govern both sustained pulse and short-pulse experiments and that deviations from this criterion in the initiation data implies that 1D conditions are no longer dominant. If the flyer diameter were too small for 1D conditions, then resulting initiation data would be to the right and/or above the estimate. The initiation curve predicted by the criterion is sensitive to the Hugoniot, and it is noTable that the Hugoniot used in the present work on EXP-A is that reported by Lacina et al. [13] and differs significantly from more typical values reported for PBXs (The "S" term is higher and the "C_0" is lower than in typical values). The attenuation criterion also provides a physical basis for the "one fifth rule" that has been observed to link the Pop-plot and the initiation curve and stems from the work of James in correlating the Pop-plot to the ignition behavior [18] where he found a factor of between 0.22 and 0.31 linking the time scales of the two plots. It can be seen by inspection of Figure 7 that τ is approximately 25 % of t_c., in excellent agreement with the reported factor. Solving Figure 7 for t_c rather than x_c and rearranging, it is found that $\tau/t_c = 1\text{-}(U_R/U_s)$, and so the "one fifth" rule amounts to assuming a constant $U_R/U_s = 1.25$, and a "one fourth rule" amounts to a ratio of 1.33. Such a distinction is probably approaching the useful limits of such an estimation. Notably, the fixed ratio of 1.3 that is found for EXP-A amounts to a "1/4.33 rule". Using typical Hugoniot parameters for PBX variants in this framework results in a ratio of almost exactly one-fifth (not shown). In any case, the proposed attenuation criteria provides a much-needed physical basis for the observed scaling linkage.

The question of applicability to other explosive formulations naturally arises. Based on the arguments just presented, any explosive for which a single scaling is observed amounts to using a constant U_R/U_s ratio in the criterion proposed here. For example, in the work of James [18], the scaling factor for PBX 9404 (a pressed HMX explosive) was reported as 0.23, amounting to $U_R/U_s = 1.30$, and PBX 9502 (a pressed TATB formulation) was reported as 0.31, or U_R/U_S of 1.43. The higher value for PBX 9502 is attributed to the complex Hugoniot of 9502 [6] and the fact that the data in the work of James (and all initiation work on 9502) is obtained above a poorly-understood kink in the Hugoniot, complicating simple estimations of release wave speed. However, for RDX/HMX formulations with simpler unreacted equations of state, a fixed ratio of 1.3 appears adequate and justified based on estimates of release wave speed.

4.3 Application of Attenuation Criterion

The application of the attenuation criterion can shed some light on recent observations of extended run distances at input pulse durations near the critical threshold. In the data of Lacina et al. [13], short pulses were used with embedded electromagnetic gauges to record gradual pulse buildup. In one of the shots (FY20-12), the short pulse input (approximately 600 ns) at almost 9 GPa is sufficient to achieve a run distance unchanged from the steady sustained-pulse run distance. In two other short pulse experiments from that work, (FY20-13 at 5 GPa and FY20-15 at 5.5 GPa) the input pressures were sufficiently low that despite indications that the explosive was building to detonation, it was clear that the run distance to reach detonation was significantly greater than the distance for a sustained pulse of equal magnitude.

Further analyzing the data from that work, if the remaining distance to detonation depends only on the shape of the current pulse (which is reasonable once the waveform is "building" and not attenuating, but is still reasonably flat-topped, and is supported by the findings of James and Lambourn on thin pulses [19]), and if the waveform is approximated as a constant velocity input, then the waveform at 10 mm (the last position recorded) can be used to approximate the pulse and roughly estimate the remaining distance required for run-up. For clarity, x* will denote the (extended) run distance from a short pulse and is always greater than or equal to x_D from a sustained pulse. For FY20-13, using a particle velocity of 0.87 km/s at a depth of 10 mm, a 5.77 GPa input pressure is calculated and so approximately 9 mm of additional run distance is required before SDT, for a total x* of 19 mm with an original input pulse of 4.98 GPa. For FY20-15, using 8.5 GPa (corresponding to a particle velocity of 1.1 km/s) as the magnitude of the input pulse at 10 mm, an estimate of remaining run distance is 4–5 mm, for a x* of 14.5 mm at 5.45 GPa.

It is straightforward to conclude that as the pulse duration decreases toward the critical threshold value, the run distances x* can grow considerably from those of the sustained pulse experiments. Using the attenuation criterion, it

is possible to quantify these effects in an effort to understand the implication of marginal pulse inputs on run distances. Figure 9 shows a plot of pressure vs run distance to detonation (x_D) for EXP-A. The solid line is the fit to the sustained pulse data as reported by Lacina, and denoted here as $\tau = \infty$ to emphasize the effectively infinite time duration of the sustained pulse loading condition. The critical threshold time from the attenuation criterion described above is τ_c, and the input time for each experiment is normalized by this critical time. The x* data from the three short pulse experiments of Lacina are plotted, using the methodology previously described to estimate the run distances. From inspection of the figure, it is reasonable to conclude that if initiation is just at the threshold, the run distance will be twice that predicted from the input pressure and Pop-plot. As the length of the input pulse increases beyond τ_c, the run distance quickly drops to that of the steady state. Once the input pulse is 2.3 τ_c, the run distance is the same as if the pulse were sustained.

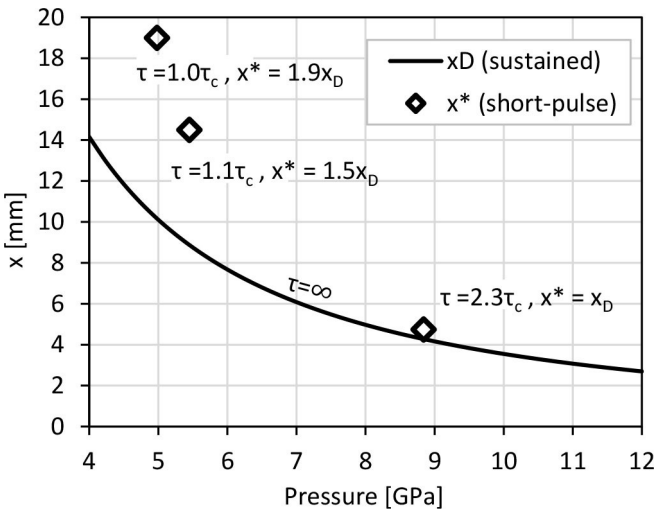

Figure 9. Run-to-detonation distance (x_D) vs input pressure for EXP-A. The solid curve is the Pop-plot fit reported by Lacina et al. [13] The data points are from the short-duration (non-sustained pulse) experiments in that work, further analyzed to estimate x_D and to present the input pulse time τ as a factor of τ_c and x_D as a factor of $x_{D,sustained}$.

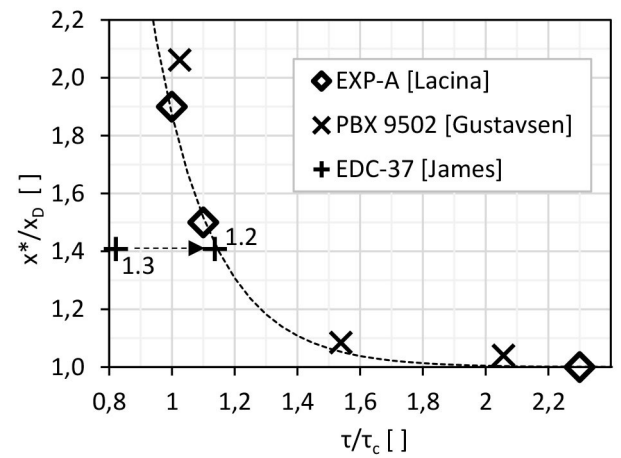

Figure 10. Normalized run distance as a function of normalized input pulse length with a suggested exponential decay to the sustained pulse values.

These data can be normalized to their respective critical values for each input pressure and considered in the framework proposed by Welle [16], which was developed to interpret computational investigations of short-pulse TATB initiation [20]. The normalized data are also shown in Figure 9, and are plotted along with an assumed exponential fit in Figure 10. The exponential decay implies that the run distance is within 10% that of the steady state value once the input pulse duration is 1.4 τ_c and within 1% by 1.9 τ_c. This observation is based on limited data and more work is required to evaluate general applicability, but the above analysis provides a framework to inform discussions of the interplay between initiation and run distance.

Other data from the literature that can be examined in the framework of Figure 9 is very sparse. Gustavsen et al. [6] reported three experiments on PBX 9502 with "short shocks". The summarized parameters, along with normalized input pulse lengths and run distances, are shown in Table 3 and plotted in Figure 10. The results agree well with those shown for EXP-A. The lone other available data point is from James and Lambourn [19] where a single "thin pulse" data point on EDC-37 was reported. Using Hugoniot and Pop-plot data for EDC-37 from [21] with experimental parameters from the paper to calculate the necessary information, the length of the input pulse was only 0.82 τ_c, yet the explosive was building to detonation (as shown in Figure 17 of [19]). Insufficient details are given, but a rough estimation from the figures suggest that detonation was imminent and would have occurred by 15 mm (only ~1.4x_D). This data point does not agree with the findings presented thus far and is shown by the far left data point in Figure 10.

However, the normalized input pulse length, with parameters for EDC-37, is very sensitive to small variation in the release wavespeed assumed. Noting the previously discussed difficulty with estimating the release speed of TATB, if the assumed U_R/U_s ratio is changed to 1.2 (from 1.3), then the normalized pulse length increases to 1.14 τ_c, again bringing the data point into good agreement (shown by the arrow from the two data points labeled "1.3" and "1.2") and building the case that the framework proposed here provides a useful physical rationale for the scaling previously reported. Broadly, the analysis suggests that until τ/τ_c falls below 1.5, there is no appreciable increase in x_D, but as τ/τ_c approaches unity, the run distance approaches 2x the sustained pulse run distance for that input pressure. As more data becomes available, the authors anticipate a bet-

Table 3. Reported parameters for thin pulse data from the literature, along with calculated values informed by the attenuation criterion. PBX9502 from [6], EDC37 data from [19].

ShotID	impactor –, mm	Target HE	V_{imp} km/s	P GPa	τ μs	x_D mm	$x_{D,ss}$ mm	$x_D/x_{D,ss}$ –	τ_c μs	τ/τ_c –
2S-97	KelF, 1.604	PBX9502	2.833	14.04	0.54	5.9	5.67	1.04	0.31*	2.24
2S-100	KelF, 1.2	PBX9502	2.832	14.04	0.35	6.15	5.67	1.08	0.31*	1.45
2S-105	KelF, 0.82	PBX9502	8.817	13.92	0.27	12†	5.82	2.06	0.32*	1.09
1279	KelF, 1.024	EDC37	1.321	4.45	0.58	15∓	10.65	1.41	0.71	0.82**

*For calculation of the input pulse length τ_c, values used were the reported (measured) pulse durations and $U_R = 1.3\ U_S$. Using 1.42 (the factor for PBX9502 reported by James) and/or calculating the impulse time from the impactor thickness and material as was done for all other experiments changes the details of the data shown here but not the qualitative larger conclusion.
†The work only reported the run distance as ">10.5 mm", but inspection of the reported data clearly shows that the run-up was nearly complete and is estimated to be 12 mm.
∓The work does not report run a run distance for this shot, but by inspection of the published Figure x_D is estimated as 14–15 mm.
**$U_R/U_S = 1.3$ was used for consistency here. Using a value of 1.2 changes τ/τ_c to 1.14.

ter understanding of the wider applicability of the framework and hope that a generic three-dimensional representation of pressure, x_D, and τ may emerge.

5 Conclusions

In summary, flyer-plate impact experiments were designed such that short duration pressure pulses were imparted onto EXP-A explosive specimens in an effort to identify critical ignition criteria. Experiments were designed to impart similar loading to that of the more common exploding foil test, but with more precisely known impact conditions and with sustained 1D strain boundary conditions. Pulse duration between shock loading and subsequent release was controlled through the implementation of a thin aluminum sheet as an impactor. Using this flyer-plate impact approach, the result was near ideal one-dimensional pulse wave input with no edge effects and a range of pressure and pulse duration combinations dependent only on impact velocity and impactor sheet thickness.

Ten experiments were conducted in an effort to observe the "Go" or "No–Go" detonation result for a given impactor thickness, varying impact velocity until a threshold was observed, with results plotted in HJ space. Data was specifically compared against exploding foil results and were found to be in good agreement. This agreement both validates our results and also indicates that 1D initiation is dominating in the EFI experiments. Furthermore, the flyer-plate impact approach demonstrates unique suitability to explore ignition conditions unavailable to EFI and to do so with greater confidence associated with well-characterized tilt metrics and impactor geometry.

Finally, a novel, physically-based initiation criterion was proposed to link the Pop-plot and the initiation curve. The criterion is termed the "attenuation criterion", and imposes a phenomena occasionally reported in sustained-pulse work as the initiation criterion. Using a single fitting parameter (an effective release wave speed) with an intuitive physical justification, the criterion provides a simple linkage to allow estimation of the initiation curve from the Pop-plot and Hugoniot data, and it is shown that the criterion works well for EXP-A. Although limited data beyond EXP-A is available, the relationship suggested is likely applicable for many explosive formulations. The value of the fitting parameter is shown to change across explosive types (for TATB vs HMX) but limited data suggests it may be constant for a range of HMX/RDX formulations. Finally, the criterion is applied to the limited data available to suggest the effect of marginally exceeding the threshold criterion on the run distance, and it is shown that the framework for estimating the interplay between run distance, input pressure, and pulse duration may also be generally applicable.

Acknowledgements

The authors thank Dr. David Lacina for providing data, discussion, and key measurements from his related work. We also thank Drs. Ben Wilde and Eric Welle for helpful discussions and encouragement and also for providing explosive samples. Approved for public release; distribution unlimted (96TW-2020-0100).

References

[1] P. Cooper, Explosives Engineering, John Wiley & Sons, 1996.
[2] H. James, Critical Energy Criterion for the Shock Initiation of Explosives by Projectile Impact, *Propellants Explos. Pyrotech.* **1988**, *13*, 35–41, 1988.
[3] H. James, An Extension to the Critical Energy Criterion Used to Predict Shock Initiation Thresholds, *Propellants Explos. Pyrotech.* **1996**, *21*, 8–13, 1996.
[4] J. Dick, Short pulse initiation of a plastic-bonded TATB explosive, *J. Energ. Mater.* **1987**, *5*, 267–285.
[5] M. Bowden, Short Duration Shock Initiation of Detonator Explosives, in *15th International Detonation Symposium*, San Francisco, CA, **2014**, pg 584.
[6] R. Gustavsen, S. Sheffield, R. Alcon, Measurements of shock initiation in the tri-amino-tri-nitro-benzene based explosive

PBX9502: Wave forms from embedded gauges and comparison of four different material lots, *J. Appl. Phys.* **2006**.
[7] H. Kleinhan, B. F. LungenstraB, H. Zollner, Initiation Threshold of High Explosives in Small Flyer Plate Experiments, in *9th Symposium on Detonation* **1989**, *66*.
[8] C. Honodel, J. Humphrey, R. Weingart, R. Lee, P. Kramer, "Shock Initiation of TATB Formulations," in *Proceedings of the 7th Symposium (International) on Detonation*, Annapolis, MD, **1981**, pp. 425.
[9] C. May, C. Tarver, Modeling Short Shock Pulse Duration Initiation of LX-16 and LX-10 Charges, in *Shock Compression of Condensed Matte*r, **2009**, pp. 275.
[10] C. Tarver, C. May, Short Pulse Shock Initiation Experiments and Modeling on LX-16, LX-10, and Ultrafine TATB, in *14th International Detonation Symposium*, **2010**, pp. 648.
[11] R. Weingart, R. Lee, R. Jackson, N. Parker, Acceleration of Thin Flyers by Exploding Metal Foils: Application to Initiation Studies, in *Proceedings of the 6th Symposium (International) on Detonation* **1976**, pp. 653.
[12] B. Trott, R. Jung, Effect of Pulse Duration on the Impact Sensitivity of Solid Explosives, in *5th Symposium (International) on Detonation*, Pasadena, CA, **1970**, pp. *191*.
[13] D. Lacina, B. Wilde, C. Neel, Shock and Detonation Response of EXP-A measured with Embedded Electromagnetic Gauges, **2020** (in preparation).
[14] O. Strand, Compact system for high-speed velocimetry using heterodyne techniques, *Rev. Sci. Instrum.* **2006**, *77*.
[15] B. J. Jensen, Accuracy limits and window corrections for photon Doppler velocimetry, *J. Appl. Phys.* **2007**, *101*.
[16] E. Welle, *Personal Communication* **2020**.
[17] J. W. Forbes, Shock Wave Compression of Condensed Matter - A Primer, Springer-Verlag, **2012**.
[18] H. R. James, Links between macroscopic behaviour and explosive morphology in shock to detonation transitions, in *13th International Detonation Symposium*, Norfolk, VA, **2006**.
[19] H. James, B. Lambourn, On the systematics of particle velocity histories in the shock-to-detonation transition regime, *J. Appl. Phys.* **2006**, *100*, 084906.
[20] R. Dorgan, G. Butler, E. Welle, "Reactive Burn Model Optimization Incorporating Ignition and Sustained Pulse Data Sets," in *Proceedings of the Fifteenth Symposium (International) on Detonation, July 2014.*.
[21] R. Gustavsen, S. Sheffield, L. Hill, R. Winter, D. Salisbury, P. Taylor, Initiation of EDC-37 Measured With Embedded Electromagnetic Particle Velocity Gauges, *11th Conference of the American Physical Society Topical Group on Shock Compression of Condensed Matter,* Snowbird, Utah (USA), June 27–July 2, **1999**, AIP Conference Proceedings 505, p. 879.

Manuscript received: April 13, 2020
Revised manuscript received: June 1, 2020
Version of record online: October 21, 2020